Forensic medical assessment of cerebral infarction, hemorrhagic hemorrhages of traumatic genesis and determination of the duration of their formation methods of spectral-selective laser-induced direct polarization-phase tomography

M.S. Garazdyuk[1], V.T. Bachinsky[1], Yu.A. Ushenko[2], P.A. Gorodenskiy[2], V.K. Gantyuk[2], M.M. Slyotov[2], I.V. Fesiv[2], Hulei[1] L, Oliinyk[1] I.
[1] Bukovinian State Medical University, Chernivtsi, Ukraine
[2]Chernivtsi National University, Chernivtsi, Ukraine

ABSTRACT

The structural-logical diagram and research design by the methods of polarization-phase tomography of linear dichroism of the polycrystalline structure [1-5] of histological sections of the brain are presented. Differential diagnosis of the formation of hemorrhages of traumatic genesis, cerebral infarction of ischemic and hemorrhagic genesis by the method of differential Mueller-matrix mapping of amplitude anisotropy - linear dichroism maps (ALD) of histological brain sections and operational characteristics of the method of their statistical analysis.
Differential diagnosis of the prescription of the formation of hemorrhages of traumatic genesis, cerebral infarction, ischemic and hemorrhagic genesis by the method of differential Mueller-matrix mapping of amplitude anisotropy - temporal dynamics of changes in the statistical structure of ALD maps of histological brain sections.

Keywords: polarization, optical anisotropy, linear dichroism, Mueller's matrix, statistical moments of the 1st-4th orders, hemorrhages of traumatic origin, cerebral infarction of ischemic and hemorrhagic genesis.

1. STRUCTURAL AND LOGICAL DIAGRAM OF POLARIZATION-PHASE TOMOGRAPHY OF THE POLYCRYSTALLINE STRUCTURE OF HISTOLOGICAL SECTIONS OF BRAIN

<table>
<tr><td colspan="4">Histological sections of the brain of the deceased</td></tr>
<tr><td>Control group deceased (group 1)</td><td>Hemorrhage of traumatic genesis (group 2)</td><td>Cerebral infarction of ischemic genesis (group 3)</td><td>Cerebral infarction of hemorrhagic genesis (group 4)</td></tr>
<tr><td colspan="4">Mueller-matrix mapping of maps of elements of 1st order differential matrix [6,7]</td></tr>
<tr><td colspan="4">Algorithms for reconstructing the distributions of average values of parameters of amplitude anisotropy</td></tr>
<tr><td colspan="4">Linear dichroism maps (ALD)</td></tr>
<tr><td colspan="4">Statistical analysis of ALD maps</td></tr>
<tr><td colspan="4">Average values and standard deviations of the magnitude of the statistical moments of the 1st - 4th orders, which characterize the coordinate distributions of the ALD value</td></tr>
<tr><td colspan="4">Criteria for differential diagnosis of samples of histological sections of the brain of the deceased from groups 1 - 4</td></tr>
<tr><td colspan="4">Time dynamics of changes in the value of statistical moments of the 1st - 4th orders, which characterize the coordinate distributions of the ALD value</td></tr>
<tr><td colspan="4">Duration of formation of hemorrhages of traumatic genesis, cerebral infarction of ischemic and hemorrhagic genesis by methods of polarization-phase tomography [8-12]</td></tr>
</table>

Fig. 1. Structural and logical diagram of polarization-phase tomography of histological sections of the brain

Fifteenth International Conference on Correlation Optics, edited by Oleg V. Angelsky, Proc. of SPIE Vol. 12126, 1212621
© 2021 SPIE · 0277-786X · doi: 10.1117/12.2616659

2. DIFFERENTIAL DIAGNOSIS OF THE FORMATION OF HEMORRHAGES OF TRAUMATIC GENESIS, CEREBRAL INFARCTION ISCHEMIC AND HEMORRHAGIC GENESIS BY THE METHOD OF POLARIZATION-PHASE REPRODUCTION OF LINEAR DICHROISM

A series of fragments in Fig. 2 shows the results of studying the coordinate (fragments (1), (3), (5), (7)) and histograms (fragments (2), (4), (6), (8)) distributions of the linear dichroism value of fibrillar networks of the nervous brain tissue with various types of pathology.

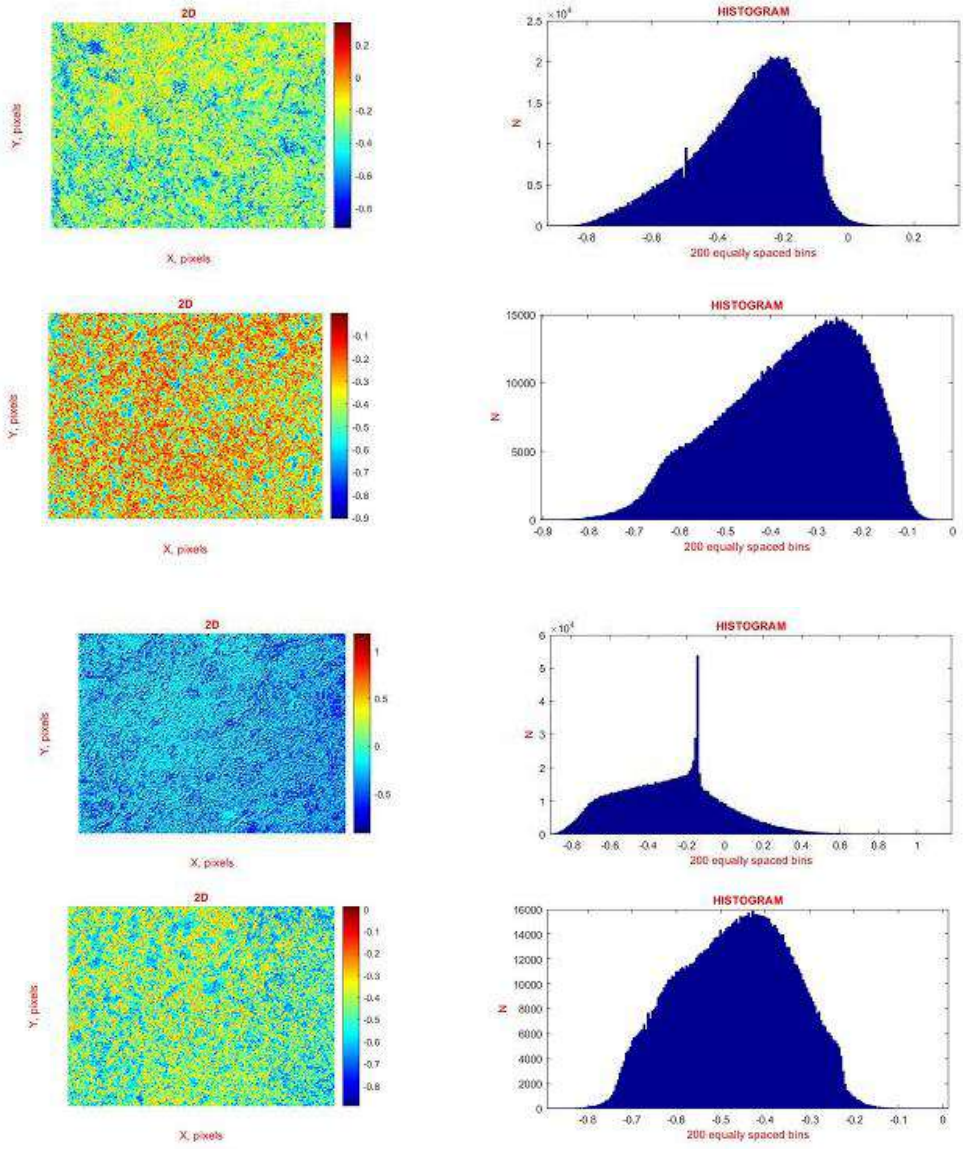

Fig. 2. Maps ((1), (2), (3), (4)) and histograms ((4), (5), (6), (7)) of the distribution of the ALD value of histological sections of the brain of the deceased from group 1 ((1), (5)), group 2 ((2), (6)), group 3 ((3), (7)) and group 4 ((4), (8)).

Analysis of polarization-reconstructed ALD maps revealed:

- individual topographic structure of all ALD maps of histological sections of the nervous tissue of the brain of the deceased from groups 1 - 4 (Fig. 2, fragments (1), (3), (5), (7));
- The histograms characterizing the distributions of the linear dichroism value of the fibrillar networks of the brain nervous tissue samples from the control 1 and research groups 2 - 4 are characterized by maximum differences in the average value SM_1, the spread of random values (dispersion SM_2), significant skewness (SM_3) and sharpness (kurtosis SM_4) of the peak (Fig. 5.4, fragments (2), (4), (6), (8)).

Table 1 presents the data of the statistical analysis of ALD maps - the mean values and errors ($\pm\Omega$) for determining the set of statistical moments of the 1st - 4th orders $SM_{i=1-4}$, characterizing the distributions of the linear dichroism value of the nervous tissue of the brain.

Table 1 Statistical moments of the 1st - 4th orders, characterizing the distributions of the ALD value of histological sections of the brain of groups 1 – 4

Parameters	Group 1	Group 2	Group 3	Group 4
SM_1	$0{,}18 \pm 0{,}008$	$0{,}24 \pm 0{,}011$	$0{,}31 \pm 0{,}014$	$0{,}39 \pm 0{,}017$
p_1		$p \prec 0{,}05$	$p \prec 0{,}05$	$p \prec 0{,}05$
p_2		$p \prec 0{,}05$		$p \prec 0{,}05$
p_3		$p \prec 0{,}05$	$p \prec 0{,}05$	
p_4		$p \prec 0{,}05$		
SM_2	$0{,}33 \pm 0{,}015$	$0{,}39 \pm 0{,}018$	$0{,}45 \pm 0{,}021$	$0{,}51 \pm 0{,}023$
p_1		$p \prec 0{,}05$	$p \prec 0{,}05$	$p \prec 0{,}05$
p_2		$p \prec 0{,}05$		$p \prec 0{,}05$
p_3		$p \prec 0{,}05$	$p \prec 0{,}05$	
p_4		$p \prec 0{,}05$		
SM_3	$0{,}65 \pm 0{,}031$	$0{,}77 \pm 0{,}035$	$0{,}91 \pm 0{,}042$	$1{,}11 \pm 0{,}052$
p_1		$p \prec 0{,}05$	$p \prec 0{,}05$	$p \prec 0{,}05$
p_2		$p \prec 0{,}05$		$p \prec 0{,}05$
p_3		$p \prec 0{,}05$	$p \prec 0{,}05$	
p_4		$p \prec 0{,}05$		
SM_4	$0{,}53 \pm 0{,}023$	$0{,}91 \pm 0{,}041$	$0{,}79 \pm 0{,}036$	$1{,}18 \pm 0{,}051$
p_1		$p \prec 0{,}05$	$p \prec 0{,}05$	$p \prec 0{,}05$
p_2		$p \prec 0{,}05$		$p \prec 0{,}05$
p_3		$p \prec 0{,}05$	$p \prec 0{,}05$	
p_4		$p \prec 0{,}05$		

The results of statistical analysis of the data of polarization-phase tomography of linear dichroism maps shown in Table 1 illustrate the statistically significant difference ($p_{i=1;2;3;4} \prec 0{,}05$) between the mean values of all statistical moments of the 1st - 4th orders, which are determined within all representative samples of histological sections of the brain.

3. OPERATIONAL CHARACTERISTICS OF THE METHOD OF STATISTICAL ANALYSIS OF ALD MAPS OF HISTOLOGICAL BRAIN SECTIONS

By tomographic reproduction of ALD maps, the following parameters of the operational characteristics of force (sensitivity, specificity and balanced accuracy) of this method of reconstruction of the polycrystalline component of the nervous tissue of the brain were established:

- good (average SM_1 and dispersion SM_2 - 85% - 92% spread of ALD values) and excellent (statistical moments of higher orders $SM_3; SM_4$, which determine the skewness and sharpness of the peak of ALD distributions - 98% - 100%) balanced accuracy of differentiation of a set of representative samples of histological sections of the brain of group "1 "-" 2 + 3 + 4 ";
- satisfactory (average SM_1 and dispersion SM_2 - 80% - 84% of the spread of ALD values) and excellent ($SM_3; SM_4$ - 95% - 97%) balanced accuracy of intergroup differentiation of histological sections of the brain of group "2" (traumatic hemorrhage) - "4" (cerebral infarction of ischemic genesis) , as well as intergroup differentiation of histological sections of the brain of group "2" (traumatic hemorrhage) - "3" (cerebral infarction of hemorrhagic genesis);
- good ($SM_{3;4}$ - 90% - 94%) balanced accuracy of intergroup differentiation of histological sections of the brain of group "3" - "4".

Table2 Specificity, sensitivity, accuracy of the method of statistical analysis of ALD maps of histological brain sections

Groups“1 – 2+3+4”			
Parameters	Sensitivity, Se,%	Specificity, Sp,%	Accuracy, Ac,%
SM_1	$a=86; b=14$	$c=85; d=15$	$n=100$
	86	**85**	**85,5**
SM_2	$a=92; b=8$	$c=90; d=10$	$n=100$
	92	**90**	**91**
SM_3	$a=100; b=0$	$c=98; d=2$	$n=100$
	100	**98**	**99**
SM_4	$a=100; b=0$	$c=98; d=2$	$n=100$
	100	**98**	**99**
Groups “2 – 3”			
Parameters	Sensitivity, Se,%	Specificity, Sp,%	Accuracy, Ac,%
SM_1	$a=82; b=18$	$c=80; d=20$	$n=100$
	82	**80**	**81**
SM_2	$a=84; b=16$	$c=81; d=19$	$n=100$
	84	**81**	**82,5**
SM_3	$a=96; b=4$	$c=95; d=5$	$n=100$
	96	**95**	**95,5**
SM_4	$a=97; b=3$	$c=95; d=5$	$n=100$
	97	**95**	**96**
Groups “2 – 4”			
Parameters	Sensitivity, Se,%	Specificity, Sp,%	Accuracy, Ac,%
SM_1	$a=83; b=17$	$c=81; d=19$	$n=100$
	83	**81**	**82**
SM_2	$a=85; b=15$	$c=83; d=17$	$n=100$

	85	**83**	**84**
SM_3	$a=97; b=3$	$c=95; d=5$	$n=100$
	97	**95**	**96**
SM_4	$a=96; b=4$	$c=95; d=5$	$n=100$
	96	**95**	**95,5**
Groups "3 – 4"			
Parameters	Sensitivity, Se,%	Specificity, Sp,%	Accuracy, Ac,%
SM_1	$a=80; b=20$	$c=78; d=22$	$n=100$
	80	**78**	**79**
SM_2	$a=78; b=22$	$c=77; d=23$	$n=100$
	78	**77**	**77,5**
SM_3	$a=92; b=8$	$c=90; d=10$	$n=100$
	92	**90**	**91**
SM_4	$a=94; b=16$	$c=92; d=8$	$n=100$
	94	**92**	**93**

4. DIFFERENTIAL DIAGNOSIS OF THE AGE OF THE FORMATION OF HEMORRHAGES OF TRAUMATIC GENESIS, CEREBRAL INFARCTION OF ISCHEMIC AND HEMORRHAGIC GENESIS BY THE METHOD OF REPRODUCING ALD DISTRIBUTIONS

In fig. 3 - fig. 5 shows maps (fragments (1), (3)) and histograms of distributions (fragments (2), (4)) of the magnitude of circular birefringence of samples of histological sections of the nervous tissue of the brain of the deceased of all groups.

Tables 3 - 5 show the results of a statistical analysis of temporary changes in necrotic changes in the structure of ALD maps of the nervous tissue of the brain of the deceased within the representative samples of samples from group 2 (table 3), group 3 (table 4) and group 4 (table 5) with different AOD (antiquity of onset of death).

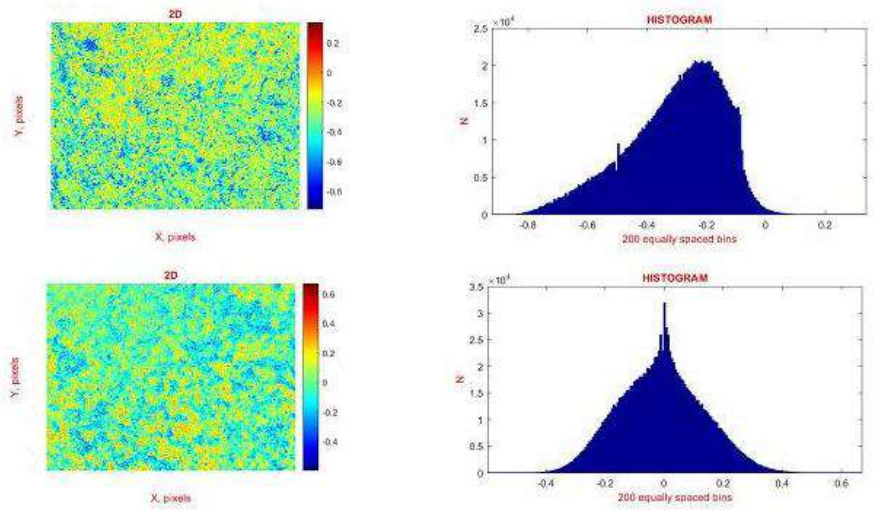

Fig. 3. Maps ((1), (2)) and histograms ((3), (4)) of the distribution of the ALD value of histological sections of the brain of the deceased from group 2 for AOD 6 hours. ((1), (3)) and AOD 24 hours ((2), (4)).

Table 3 Time dynamics of changes in the statistical moments of the 1st - 4th orders characterizing the distributions of the ALD value of histological brain sections of the deceased from group 2

T, **hours**	**6**	**12**	**18**	**24**	**48**
SM_1	$0,24 \pm 0,008$	$0,22 \pm 0,007$	$0,205 \pm 0,006$	$0,19 \pm 0,005$	$0,16 \pm 0,005$
p	$p \prec 0,05$				
SM_2	$0,41 \pm 0,014$	$0,37 \pm 0,013$	$0,35 \pm 0,013$	$0,33 \pm 0,012$	$0,25 \pm 0,01$
p	$p \prec 0,05$				
SM_3	$0,91 \pm 0,034$	$1,39 \pm 0,054$	$1,63 \pm 0,072$	$1,87 \pm 0,088$	$2,83 \pm 0,11$
p	$p \prec 0,05$				
SM_4	$0,78 \pm 0,031$	$1,33 \pm 0,059$	$1,58 \pm 0,065$	$2,79 \pm 0,11$	$2,91 \pm 0,12$
p	$p \prec 0,05$				
T, **hours**	**72**	**96**	**120**	**144**	**168**
SM_1	$0,11 \pm 0,004$	$0,08 \pm 0,003$	$0,09 \pm 0,004$	$0,08 \pm 0,003$	$0,07 \pm 0,003$
p	$p \prec 0,05$		$p \succ 0,05$		
SM_2	$0,17 \pm 0,006$	$0,11 \pm 0,004$	$0,12 \pm 0,004$	$0,11 \pm 0,004$	$0,12 \pm 0,004$
p	$p \prec 0,05$		$p \succ 0,05$		
SM_3	$3,73 \pm 0,31$	$4,51 \pm 0,32$	$4,66 \pm 0,32$	$4,12 \pm 0,31$	$4,39 \pm 0,31$
p	$p \prec 0,05$		$p \succ 0,05$		
SM_4	$3,98 \pm 0,23$	$4,71 \pm 0,25$	$4,88 \pm 0,26$	$4,56 \pm 0,22$	4.39 ± 0.21
p	$p \prec 0,05$		$p \succ 0,05$		

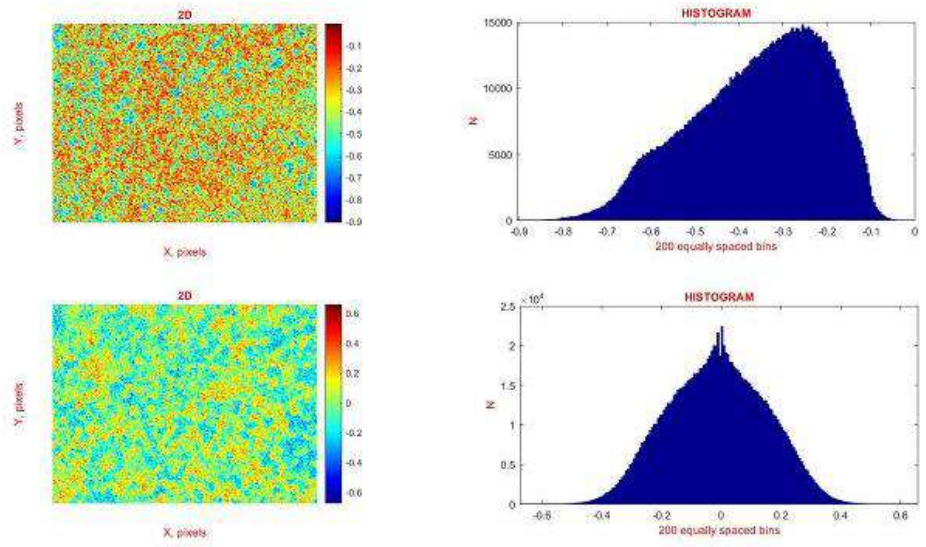

Fig. 4. Maps ((1), (2)) and histograms ((3), (4)) of the distribution of the ALD value of histological sections of the brain of the deceased from group 3 for AOD 6 hours. ((1), (3)) and AOD 24 hours ((2), (4)).

Table 4 Time dynamics of changes in the statistical moments of the 1st - 4th orders, characterizing the distribution of the ALD value of histological brain sections of the deceased from group 3

T, **hours**	**6**	**12**	**18**	**24**	**48**
SM_1	0,15 ±	0,137 ±	0,13 ±	0,12 ±	0,1 ±
p	$p \prec 0,05$				
SM_2	0,31 ±	0,28 ±	0,26 ±	0,25 ±	0,205 ±
p	$p \prec 0,05$				
SM_3	0,71 ±	1,06 ±	1,23 ±	1,41 ±	2,11 ±
p	$p \prec 0,05$				
SM_4	0,63 ±	1,06 ±	1,27 ±	1,48 ±	2,03 ±
p	$p \prec 0,05$				
T, **hours**	**72**	**96**	**120**	**144**	**168**
SM_1	0,07 ±	0,05 ±	0,06 ±	0,05 ±	0,04 ±
p	$p \prec 0,05$		$p \succ 0,05$		
SM_2	0,13 ±	0,08 ±	0,09 ±	0,08 ±	0,07 ±
p	$p \prec 0,05$		$p \succ 0,05$		
SM_3	2,79 ±	3,35 ±	3,44 ±	3,13 ±	3,27 ±
p	$p \prec 0,05$		$p \succ 0,05$		
SM_4	3,19 ±	3,81 ±	3,99 ±	3,73 ±	3,88 ±
p	$p \prec 0,05$		$p \succ 0,05$		

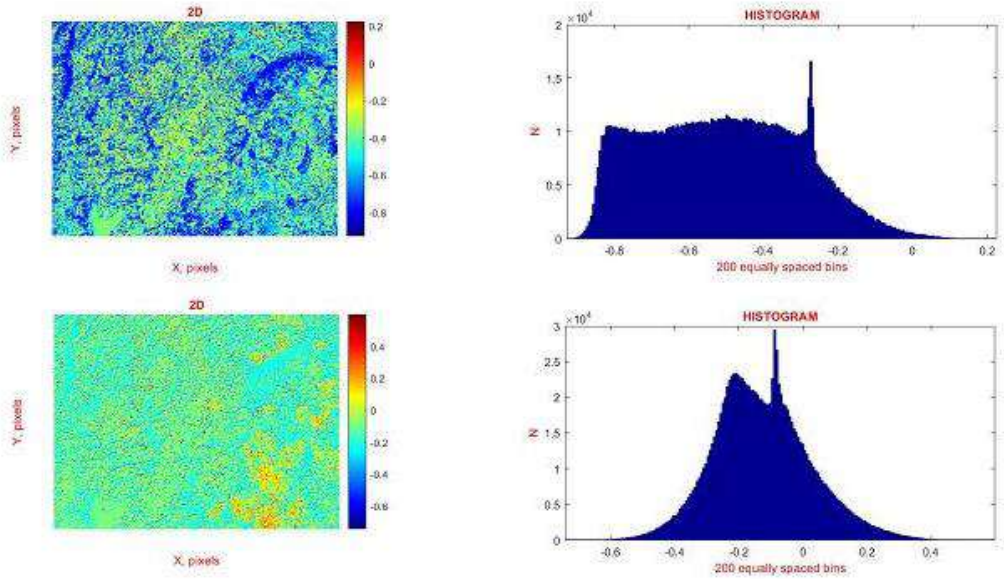

Fig. 5. Maps ((1), (2)) and histograms ((3), (4)) of the distribution of the ALD value of histological sections of the brain of the deceased from group 4 for AOD 6 hours. ((1), (3)) and AOD 24 hours ((2), (4)).

Table 5 Time dynamics of changes in the statistical moments of the 1st - 4th orders, characterizing the distribution of the ALD value of histological brain sections of the deceased from group 4

T, **hours**	**6**	**12**	**18**	**24**	**48**
SM_1	$0,21 \pm 0,006$	$0,192 \pm 0,005$	$0,18 \pm 0,005$	$0,17 \pm 0,004$	$0,14 \pm 0,003$
p	$p \prec 0,05$				
SM_2	$0,36 \pm 0,009$	$0,33 \pm 0,008$	$0,31 \pm 0,007$	$0,285 \pm 0,006$	$0,23 \pm 0,005$
p	$p \prec 0,05$				
SM_3	$0,69 \pm 0,021$	$1,09 \pm 0,029$	$1,31 \pm 0,033$	$1,52 \pm 0,055$	$2,34 \pm 0,16$
p	$p \prec 0,05$				
SM_4	$0,83 \pm 0,026$	$1,36 \pm 0,034$	$1,63 \pm 0,043$	$1,89 \pm 0,049$	$2,96 \pm 0,17$
p	$p \prec 0,05$				
T, **hours**	**72**	**96**	**120**	**144**	**168**
SM_1	$0,095 \pm 0,003$	$0,07 \pm 0,0025$	$0,08 \pm 0,003$	$0,07 \pm 0,003$	$0,09 \pm 0,004$
p	$p \prec 0,05$		$p \succ 0,05$		
SM_2	$0,16 \pm 0,004$	$0,09 \pm 0,003$	$0,1 \pm 0,004$	$0,09 \pm 0,003$	$0,08 \pm 0,003$
p	$p \prec 0,05$		$p \succ 0,05$		
SM_3	$3,17 \pm 0,16$	$3,51 \pm 0,17$	$3,57 \pm 0,17$	$3,43 \pm 0,16$	$3,51 \pm 0,17$
p	$p \prec 0,05$		$p \succ 0,05$		
SM_4	$4,03 \pm 0,1`9$	$4,88 \pm 0,21$	$4,99 \pm 0,22$	$4,76 \pm 0,21$	$4,94 \pm 0,22$
p	$p \prec 0,05$		$p \succ 0,05$		

From the analysis of the results of statistical processing of the topographic structure of tomograms of linear dichroism of fibrillar networks of histological sections of the brain (Fig. 3 - Fig. 5) of the deceased from all groups, one can see a large temporal dynamics of necrotic destruction of the nervous tissue. In accordance with this, there is a faster temporal decrease in the absolute values and the range of scatter of the linear dichroism value with increasing AOD time (Fig. 3 - Fig. 5, fragments (2), (4)).

The following regularities of the scenario of temporary changes in the topographic structure of the ALD maps have been established:

- an increase in the magnitude of the range of temporal linear changes in the values of statistical moments of the 1st - 4th orders, characterizing the distributions of the magnitude of the linear dichroism of fibrillar networks of histological sections of the nervous tissue of the brain of the deceased from all groups up to 24 hours;
- the accuracy of the AOD determination is 30 min. ± 5 min.

CONCLUSIONS

1. The design of forensic differentiation of cases of cerebral infarction, hemorrhagic hemorrhages of traumatic genesis and determination of the age of their formation by means of experimental testing of methods of polarization-phase tomography of optical anisotropy, investigated on the basis of the developed structural-logical scheme, has been substantiated.

2. The following parameters of the strength of the method of polarization-phase tomography were experimentally established:

- Linear dichroism - good (SM_1 and SM_2 - 85% - 92%) and excellent ($SM_3; SM_4$ - 98% - 100%) balanced accuracy of differentiation of a set of representative samples of histological brain sections of group "1" - "2 + 3 + 4";

satisfactory (SM_1 and SM_2 - 80% - 84%) and excellent ($SM_3; SM_4$ - 95% - 97%) balanced accuracy of intergroup differentiation of histological sections of the brain of group "2" - "4", as well as intergroup differentiation of histological sections of the brain of group "2" - "3" "; good ($SM_{3;4}$ - 90% - 94%) balanced accuracy of intergroup differentiation of histological sections of the brain of the group "3" - "4";

3. By temporarily monitoring the change in the magnitude of the statistical moments of the 1st - 4th orders, which characterize the polarization-reproduced maps of the set of mechanisms of optical anisotropy of the polycrystalline structure of the nervous tissue, the following parameters of the differential determination of the duration of the formation of cases of cerebral infarction, hemorrhagic hemorrhages of traumatic genesis were determined:

- tomography of the distributions of the linear dichroism value of histological sections of the brain – AOD 24 hours, accuracy 30 min. ± 5 min.

FUNDING

Current research supported by the National Research Foundation of Ukraine (Project 2020.02/0061)

REFERENCES

[1] S. Alali et al., "Quantitative correlation between light depolarization and transport albedo of various porcine tissues," J. Biomed. Opt. 17(4), 045004 (2012).
[2] A. Pierangelo et al., "Multispectral Mueller polarimetric imaging detecting residual cancer and cancer regression after neoadjuvant treatment for colorectal carcinomas," J. Biomed. Opt. 18(4), 046014 (2013).
[3] E. Du et al., "Mueller matrix polarimetry for differentiating characteristic features of cancerous tissues," J. Biomed. Opt. 19(7), 076013 (2014).
[4] A. Doronin, C. Macdonald, and I. Meglinski, "Propagation of coherent polarized light in highly scattering turbid media," J. Biomed. Opt. 19(2), 025005 (2014).
[5] B. Kunnen et al., "Application of circularly polarized light for non-invasive diagnosis of cancerous tissues and turbid tissue-like scattering media," J. Biophotonics 8(4), 317–323 (2015).
[6] Ushenko, V.O., Trifonyuk, L., Ushenko, Y.A., Dubolazov, O.V., Gorsky, M.P., Ushenko, A.G. Polarization singularity analysis of Mueller-matrix invariants of optical anisotropy of biological tissues samples in cancer diagnostics (2021) Journal of Optics (United Kingdom), 23 (6), 064004.
[7] Meglinski, I., Trifonyuk, L., Bachinsky, V., Vanchulyak, O., Bodnar, B., Sidor, M., Dubolazov, O., Ushenko, A., Ushenko, Y., Soltys, I.V., Bykov, A., Hogan, B., Novikova, T. Polarization Correlometry of Microscopic Images of Polycrystalline Networks Biological Layer (2021) SpringerBriefs in Applied Sciences and Technology, pp. 61-73.
[8] Angelsky, O.V., Bekshaev, A.Y., Dragan, G.S., Maksimyak, P.P., Zenkova, C.Y., Zheng, J. Structured Light Control and Diagnostics Using Optical Crystals (2021) Frontiers in Physics, 9,715045.
[9] Angelsky, O.V., Bekshaev, A.Y., Hanson, S.G., Zenkova, C.Y., Mokhun, I.I., Jun, Z. Structured Light: Ideas and Concepts (2020) Frontiers in Physics, 8, 114
[10] Ushenko, A.G. Laser Polarimetry of Polarization-Phase Statistical Moments of the Object Field of Optically Anisotropic Scattering Layers (2001) Optics and Spectroscopy (English translation of Optika i Spektroskopiya), 91 (2), pp. 313-316
[11] Angelsky, O.V., Maksimyak, P.P. Optical diagnostics of slightly rough surfaces (1992) Applied Optics, 31 (1), pp. 140-143
[12] Angelsky, O.V., Zenkova, C.Y., Hanson, S.G., Zheng, J. Extraordinary Manifestation of Evanescent Wave in Biomedical Application (2020) Frontiers in Physics, 8, 159.
[13] Angelsky, O.V., Hanson, S.G., Maksimyak, A.P., Maksimyak, P.P. On the feasibility for determining the amplitude zeroes in polychromatic fields (2005) Optics Express, 13 (12), pp. 4396-4405
[14] Ushenko, A.G., Burkovets, D.N., Ushenko, Yu.A. Polarization-Phase Mapping and Reconstruction of Biological Tissue Architectonics during Diagnosis of Pathological Lesions (2002) Optics and Spectroscopy (English translation of Optika i Spektroskopiya), 93 (3), pp. 449-456.
[15] Ushenko, A.G. Laser Polarimetry of Polarization-Phase Statistical Moments of the Object Field of Optically Anisotropic Scattering Layers (2001) Optics and Spectroscopy (English translation of Optika i Spektroskopiya), 91 (2), pp. 313-316.